

Experimental measurements of two elastic taut-slack mooring configurations for the multi-float M4 WEC

Samuel Draycott, Peter K Stansby, and Gangqiang Li

Abstract—Mooring is a vital and often problematic component of any floating offshore renewable energy system, whether for wind or wave energy conversion, and here we consider the M4 multi-float wave energy converter (WEC) system in a 122 configuration. Previous experimental work has shown elastic cables to reduce extreme snap loads by a factor of about 6 when considering single cables between the bow float and a mooring buoy (hawser), and between the mooring buoy and the bed. Here, we compare results for two alternative configurations designed to reduce the mooring footprint as well as extreme snap loads. Both systems are taut-slack with configuration 1 consisting of a single mooring buoy and configuration 2 with a dual buoy set-up with one submerged in an attempt to reduce loads further. The configurations are experimentally tested in irregular (JONSWAP) wave conditions up to limiting steepness, with run times of 35 minutes at 1:40 scale or about 3.5 hours full scale. Through statistical analysis it is concluded that both mooring configurations offer similar advantages in terms of reduction of peak loads, and display very similar load and motion (hence power) statistics. Configuration 2 displays slightly larger maximum forces yet these occur at significantly lower frequencies (near to the surge natural frequency) with reduced response at the wave frequencies. This demonstrates that subtle changes to mooring line configuration can be used to affect the frequency, and hence number, of loading cycles considerably without affecting power performance.

Index Terms—Wave energy converter, moorings, extreme waves, experimental testing

I. INTRODUCTION

WAVE energy has the potential to contribute large amounts of power to the grid with the global potential similar to offshore wind [1]. This resource, however, remains unexploited due to significant design

Part of a special issue for EWTEC 2023. Original version published in EWTEC 2023 proceedings at <https://doi.org/10.36688/ewtec-2023-485>.

Manuscript submitted 6 January 2025; Accepted 8 January 2025. Published 31 May 2025.

This is an open access article distributed under the terms of the Creative Commons Attribution 4.0 licence (CC BY <http://creativecommons.org/licenses/by/4.0/>).

This article has been subject to single blind peer review by a minimum of two reviewers.

This work was in part, funded by the EPSRC, UK, on the Moor-WEC project (EP/V039946/1).

Samuel Draycott is based at School of Engineering, University of Manchester, Manchester, UK (Samuel.Draycott@manchester.ac.uk).

Peter K Stansby is based at School of Engineering, University of Manchester, Manchester, UK (P.K.Stansby@manchester.ac.uk).

Gangqiang Li was based at School of Engineering, University of Manchester, Manchester, UK when the work was conducted but now is based at École Centrale de Nantes, Nantes, France (gangqiang.li@ec-nantes.fr).

Digital Object Identifier: <https://doi.org/10.36688/imej.8.119-125>

challenges for wave energy converters. Moorings represent one of the major remaining challenges [2] which need to provide station-keeping in extreme conditions without significantly restricting the device motion required for energy conversion [3]. This requires mooring design which deviates from more conventional ocean engineering applications.

Here we are concerned with the M4 wave energy converter (WEC) which is a hinged attenuator device designed to extract power using a multi-mode, multi-float system with capacity similar to offshore wind [4]. Previous work with the M4 device has demonstrated that a single elastic cable between a mooring buoy and the bed [5] can reduce snap loads by a factor of 6 compared with using inelastic cables [6]. Here, we experimentally assess two alternative mooring configurations using elastic cables designed to reduce the mooring footprint as well as the extreme snap loads. Both configurations use three elastic cables between the buoy and the bed in order to reduce the mooring footprint. The first configuration uses a single mooring buoy, whilst the second using a dual-buoy configuration smaller buoys the larger of which is submerged. The aim of the second configuration is to reduce the direct loading on the buoys themselves through submergence, whilst maintaining total buoyancy, and hence reducing the total loads transmitted to the anchor.

Experiments are conducted at the Ocean basin of the COAST laboratory at the University of Plymouth and we assess both mooring configurations in a range of irregular wave conditions up to limiting steepness. Statistics and spectra are presented for bed (front) mooring line force and hinge angle for both configurations.

The paper is laid out as follows. The experimental set-up is detailed in Section II including the mooring configurations and WEC set-up along with the sea state parameters. Results are presented in Section III considering basic statistics along with spectral analysis. Concluding remarks are offered in Section IV.

II. EXPERIMENTAL SET-UP

A. WEC and mooring configuration

All tests were conducted in the Ocean basin at the COAST laboratory, University of Plymouth. The water depth was set to 2 m. As depicted in Figures 1 to 5, a 1:40 scale model of the 1-2-2 multi-float M4 WEC was installed with two different mooring configurations. This system has one bow float (diameter, $D = 0.25$ m),

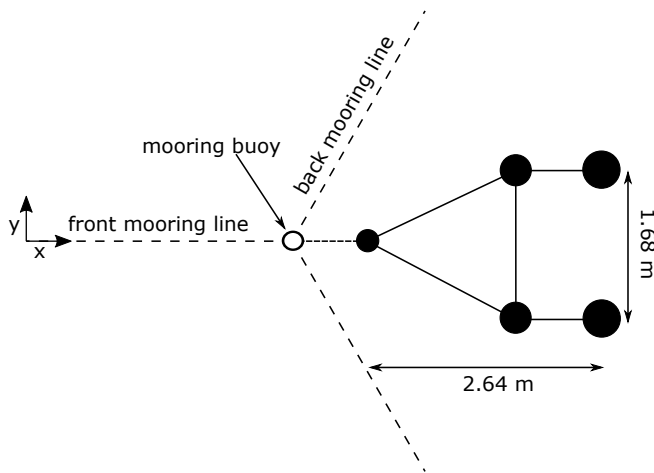


Fig. 1. Top-down diagram of M4 WEC and mooring configuration 1 (Config. 1)

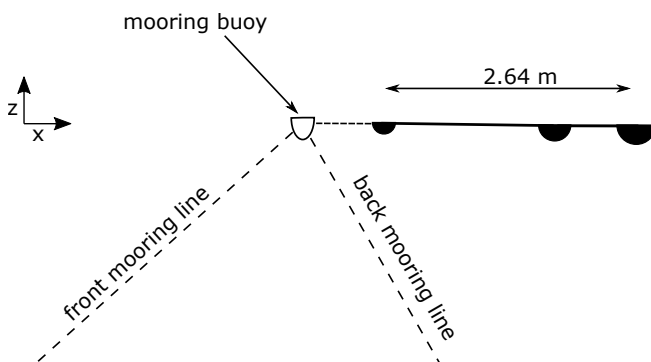


Fig. 2. Side-on diagram of M4 WEC and mooring configuration 1 (Config. 1)

two mid floats ($D = 0.35$ m) and two stern floats ($D = 0.42$ m). The bow and mid floats effectively make up a rigid frame, with the stern floats connected via a hinge, allowing power take-off based on the relative rotations. The hinge angle, θ , is defined in Figure 5 along with the float naming convention. Controllable motors are installed on the mid-floats to enable simulation of power take-off but remain unconnected throughout these tests as they investigate extreme waves where there would be no energy extraction. Each motor weighs 4.35 kg, and mid floats including ballast weigh 4.56 kg each. The bow float weighs 3.2 kg including ballast and the stern floats weigh 28.0 kg each including ballast. The beams connecting the bow to the mid floats weigh 2.52 kg (total), with beams connecting the mid floats to the stern floats weigh 3.10 kg (total). Mid-float cross beams weigh 8.3 kg (total).

Figures 1 and 2 show mooring configuration 1 (Config. 1). In this configuration a large hemispherical surface buoy is connected to the seabed with three equi-spaced elastic cables in pre-tension, with a single elastic cable to the bow float. The three mooring lines remain in tension whilst the hawser line – connecting the bow float to the mooring buoy – oscillates between being slack and in tension based on the M4 motions. The hemispherical mooring buoy is 0.2 m in diameter and 1.25 kg. The three pre-tensioned bed-mounted mooring lines are at approximately 30° to the bed plane

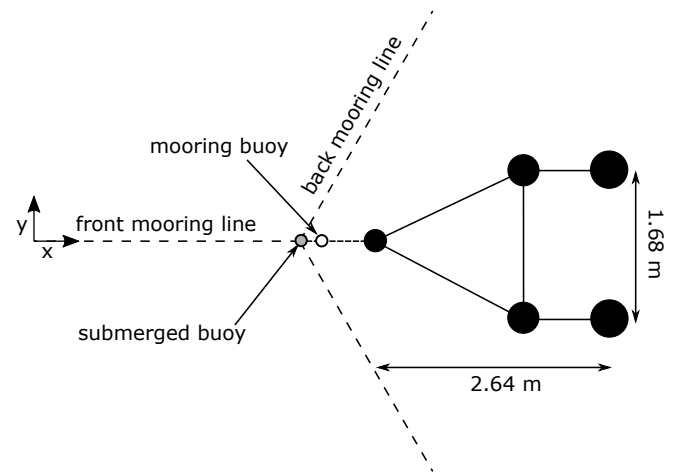


Fig. 3. Top-down diagram of M4 WEC and mooring configuration 2 (Config. 2)

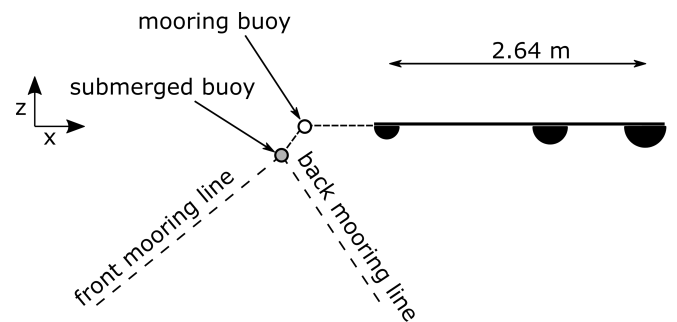


Fig. 4. Side-on diagram of M4 WEC and mooring configuration 2 (Config. 2)

and nominally 120° to each other in the $x-y$ plane. The front mooring line was 1.97 m unstretched and 3.47 m stretched, and the back mooring lines 2.50 m unstretched and 4.00 m stretched. The difference is due to available bed connection points at 1 m spacings. The mooring lines are effectively elastic cables, comprising two Allcare 0.6 m medium (red) exercise bands connected by light carabiners giving a nominal stiffness of 65 N/m. The dynamic tension–extension curve for the Allcare bands are presented in Figure 6 demonstrating hysteresis.

The second mooring configuration (Config. 2) is depicted in Figures 3 and 4 and is effectively a modification to Config. 1. In this configuration there is a smaller submerged buoy connected to the seabed with three equi-spaced elastic cables in pre-tension, however, this is connected to a smaller surface buoy which is sub-

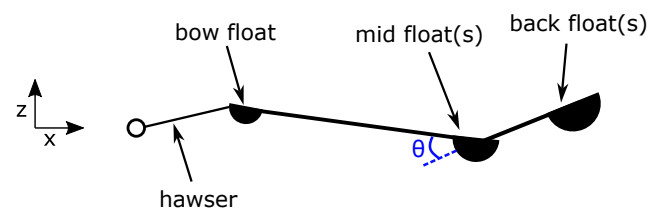


Fig. 5. Diagram defining hinge angle, θ , along with the hawser line, bow, mid, and back floats

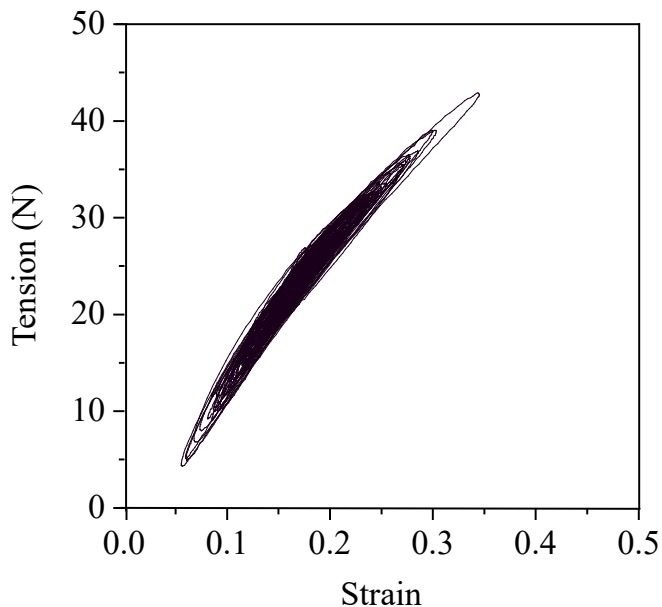


Fig. 6. Dynamic plot of tension vs strain for the Allcare medium (red) exercise bands

sequently connected to the bow float. All cables are elastic and are comprised of the same Allcare exercise bands as Config. 1. Again the mooring lines remain in tension, as does the line between the buoys, yet the hawser line is often slack. The logic behind this configuration is to reduce the mooring line loads through reduction of the loads acting directly the buoy(s) whilst providing equivalent buoyancy and hence pre-tension. The submerged buoy in this configuration is 0.15 m in diameter and 0.21 kg. The front mooring line was 2.09 m unstretched and 3.45 m when stretched, and the back mooring lines are 2.94 m unstretched and 4.0 m stretched. The difference is again due to bed connection availability. At rest, the centre of the submerged buoy is 0.16 m beneath the still water surface. The floating mooring buoy is 0.11 m diameter and 0.087 kg, and is connected to the submerged buoy by a light cord (0.38 m centre to centre), and connected to the bow float (0.68 m centre to fairlead) with a single elastic exercise band of the same type. Both configurations have line pre-tensions approximately between 13 N and 15 N.

B. Wave conditions

Eleven wave conditions are generated based on JON-SWAP spectra [7] with different values of significant wave height (H_{m0}) and peak period (T_p), with a peak enhancement factor γ of 3.3 for all conditions. These wave conditions are defined in Table 1. Sea states have a repeat time T_r of 2048 s which gives frequency increments Δf of 1/2048 Hz. Run times are set to 2100 s to ensure that there is a full stationary repeat period after all frequency components have arrived at the model position. The final T_r seconds of data is used for spectral and statistical analysis as presented in Section III.

TABLE I
TARGET WAVE CONDITIONS

ID	H_{m0}	T_p	γ
1	0.06	1.21	3.3
2	0.06	1.39	3.3
3	0.06	1.78	3.3
4	0.09	1.21	3.3
5	0.09	1.39	3.3
6	0.09	1.78	3.3
7	0.13	1.21	3.3
8	0.13	1.39	3.3
9	0.13	1.78	3.3
10	0.16	1.39	3.3
11	0.16	1.78	3.3

C. Instrumentation

For all experiments we measure mooring line loads at the bed on the front mooring line F_{front} (see Figures 1–4) using Futek submersible load cells. Six degree-of-freedom (DoF) body motions are recorded for all five floats using a Qualisys camera-based motion capture system, which we use to compute the hinge angle θ . In addition, surface elevations at three x locations are measured using resistance-type wave gauges (7.8 m, 14.8 m and 15.3 m from the wavemakers), noting that the mooring buoy (Config. 1) and submerged buoy (Config. 2) are installed at 14.4 m.

III. RESULTS

A. Statistical comparison between mooring configurations

1) *Bed forces*: Figures 7, 8 and 9 show the maximum, standard deviations and wave-induced mean bed forces as a function of H_{m0} for different values of T_p . Values are presented against measured H_{m0} calculated as $H_{m0} = 4\sqrt{\int_0^\infty S(f)df}$ where $S(f)$ is the measured energy density spectrum. Peak forces in Figure 7 are presented after removing the mean to show the dynamic load whilst mean forces in Figure 9 are given after removing the pre-tension determined at the start of each test (to account for a slow sensor drift), thus leaving the wave-induced mean force. It is evident that maxima, mean, and standard deviations are comparable for both mooring configurations, yet maxima and standard deviations are slightly higher for Config. 2. This was an unexpected result, yet both mooring configurations offer significant reduction on dynamic forces compared with an inextensible line and a single elastic line. Both configurations 1 and 2 reduce dynamic loads relative to an inelastic line [6] by around a factor of 15, and reduce dynamic loads relative to a single elastic line [5] by around a factor of 2 after accounting for model scale (according to Froude). Total loads (including wave-induced mean and pre-tension) are reduced by approximate factors of 9 and 1.3 for both configurations when compared to an inelastic and a single-elastic line respectively. It is to be noted that the conditions and WEC float configurations varied

between these experiments and so did the realisations (phases) so these values are approximate. This is still a good indication on performance as for each set of experiments, cases were generated up to limiting steepness for a range of peak periods including those close to the model natural frequencies.

Larger forces (maximum, mean and standard deviations) are evident for $T_p = 1.2$ s for equivalent values of H_{m0} due to the higher wave steepness and proximity of the dominant wave frequencies ($f_p = 1/T_p = 0.833$ Hz) to the pitch natural frequency of the mid-stern floats (approximately 0.9 Hz).

2) *Hinge angle*: Figures 10 and 11 show the maxima and standard deviations of the hinge angle θ as a function of H_{m0} for different values of T_p . Values are near-identical between both mooring configurations demonstrating that although the peak mooring line loads were larger for Config. 2 this does not affect the device motions, thus highlighting an independence on the mooring design on response and hence power output in operational conditions if sufficiently compliant.

B. Spectral analysis

Bed force spectra are presented in Figure 12 for the largest H_{m0} value for each T_p (cases 7, 10 and 11). The peak frequency for each case is indicated by the dashed blue line. There are some large differences between the spectra indicating that configuration 2 results in significantly reduced forces at the wave frequencies, yet much larger forces at around 0.07 Hz close to the surge natural frequency (expected around 0.08 Hz and indicated on the figures as a vertical black dashed line). The reasons behind this are complex and remain not fully understood. This is, however, observed for all wave conditions tested. Thus, the dual buoy configuration, despite being associated with larger peak loads, is associated with a reduction in the number of loading cycles which may be beneficial for mooring line fatigue. The mooring design should therefore be done in conjunction with fatigue testing of elastic moorings to optimise the lifetime of the mooring system.

Hinge angle spectra are presented in Figure 13 for the largest H_{m0} value for each T_p . Peaks are observed at the peak wave frequency and the pitch natural frequency indicated by dashed blue and black lines respectively. These become a single peak for $T_p = 1.2$ s and $T_p = 1.4$ s where the natural frequency in pitch closely aligns with the peak wave frequency. There is virtually no difference between the mooring configurations indicating that the mooring design and associated loading spectra do not affect the device motions and power performance, and if suitably compliant to allow motion, can be designed separately from the electro-mechanical aspects of the WEC system.

IV. CONCLUSION

It is well known that elastic mooring cables reduce snap loads compared to inelastic cables but the most effective configurations have yet to be established and quantified. Here we consider two taut-slack systems. The most obvious has a single mooring buoy at the

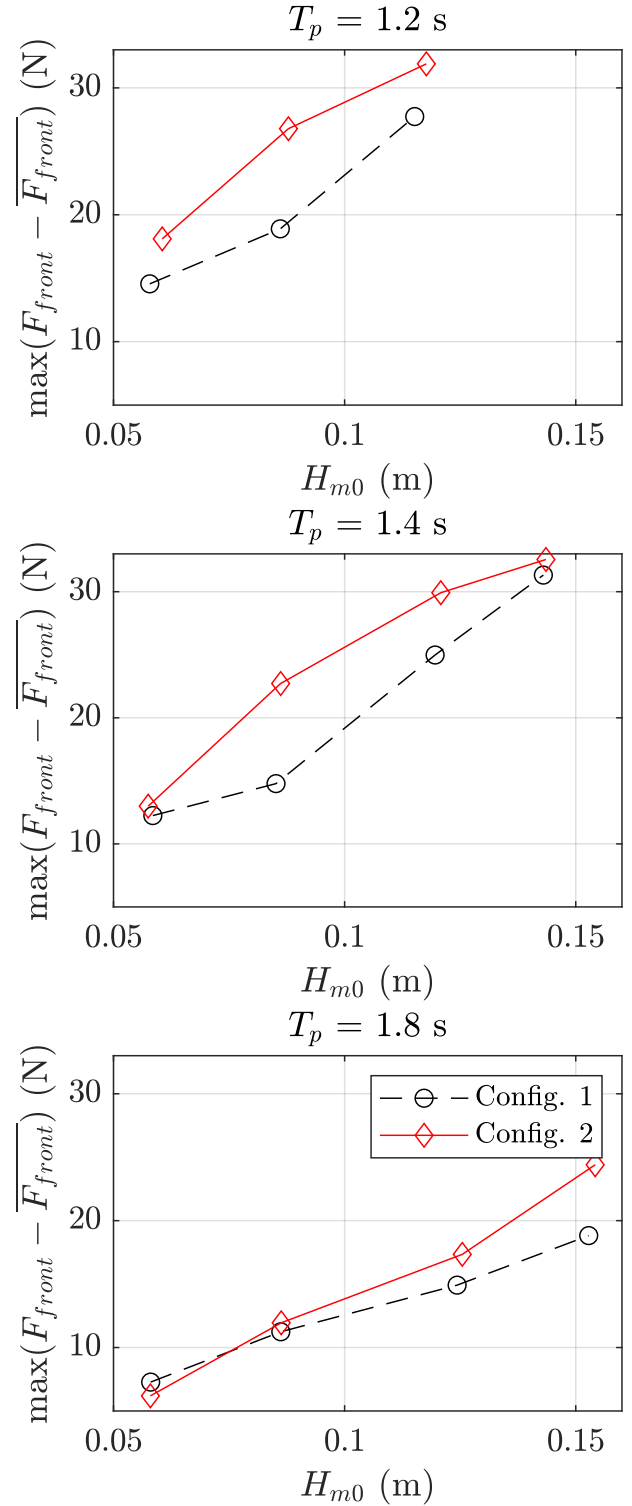


Fig. 7. Maximum bed force as a function of H_{m0} for different values of T_p

water surface attached to the bed by three elastic lines with sufficient pre-tension to avoid going slack in any wave condition. The three lines at 120° intervals limit the horizontal footprint. We consider the tension loads at the bed determining the anchor loads. The buoy is attached to the fairlead on the bow float by a hawser. This reduces snap mooring forces by a factor of about 15 below a single inextensible cable and about two below that for a single elastic cable. In an attempt

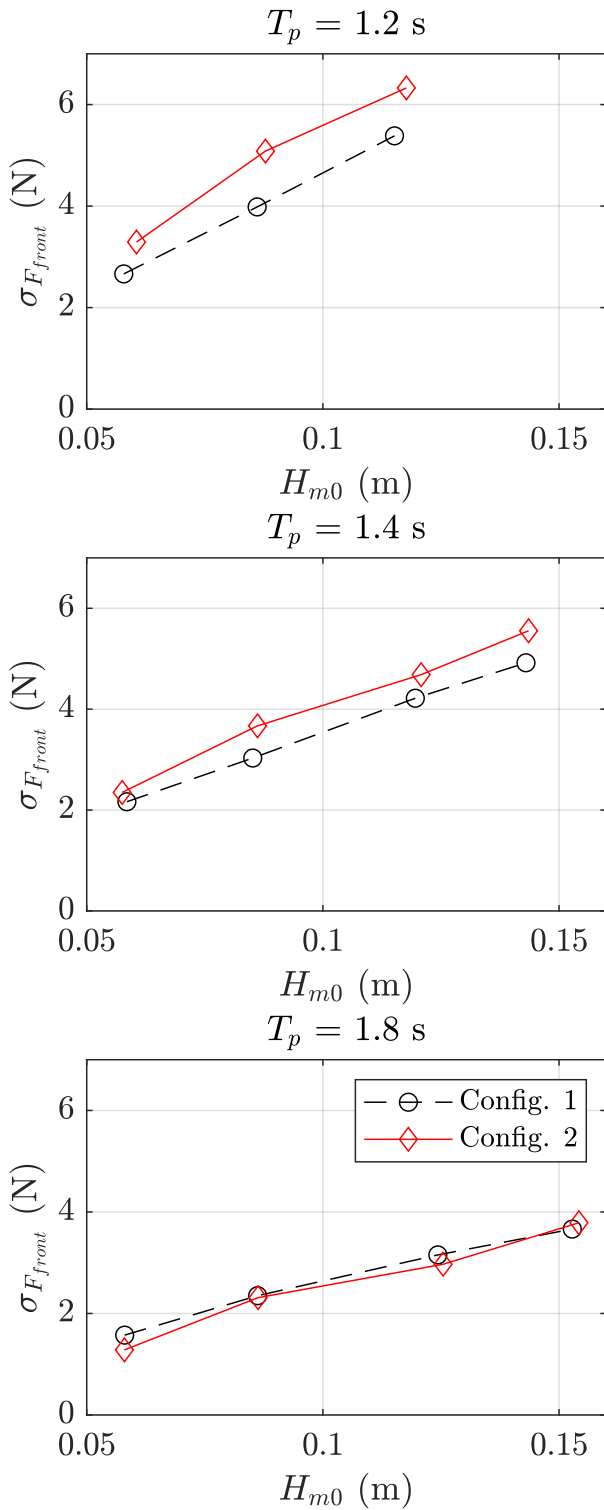


Fig. 8. Standard deviation of bed force as a function of H_{m0} for different values of T_p

to reduce loads further the three taut cables in pre-tension are attached to a submerged buoy, smaller than the single buoy, always below wave troughs, so that wave loads on the buoy will be reduced. A smaller surface buoy is attached to this buoy by a short cable and there is a hawser from the surface buoy to the fairlead on the bow float. This is thus a two-buoy taut-slack system. Counter intuitively the peak loads are slightly increased. The force spectra are also

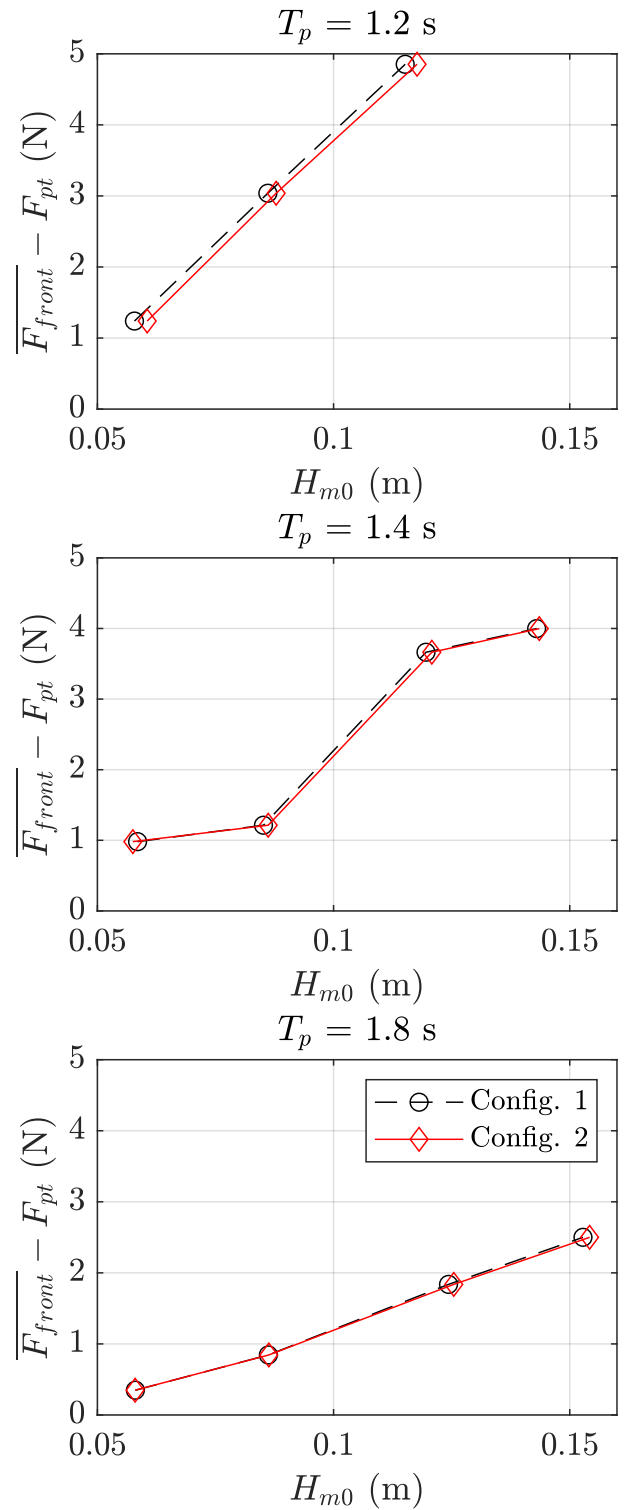


Fig. 9. Mean wave-induced bed force as a function of H_{m0} for different values of T_p

modified with reduced energy at the wave frequencies and more at the surge natural frequency which may be beneficial for fatigue life. The relative angular response between bow-mid and mid-stern floats is effectively unchanged between configurations as expected from previous experience. The elastic mooring systems are highly nonlinear and complex dynamically and there is clearly scope for further mooring optimisation as investigated by [8].

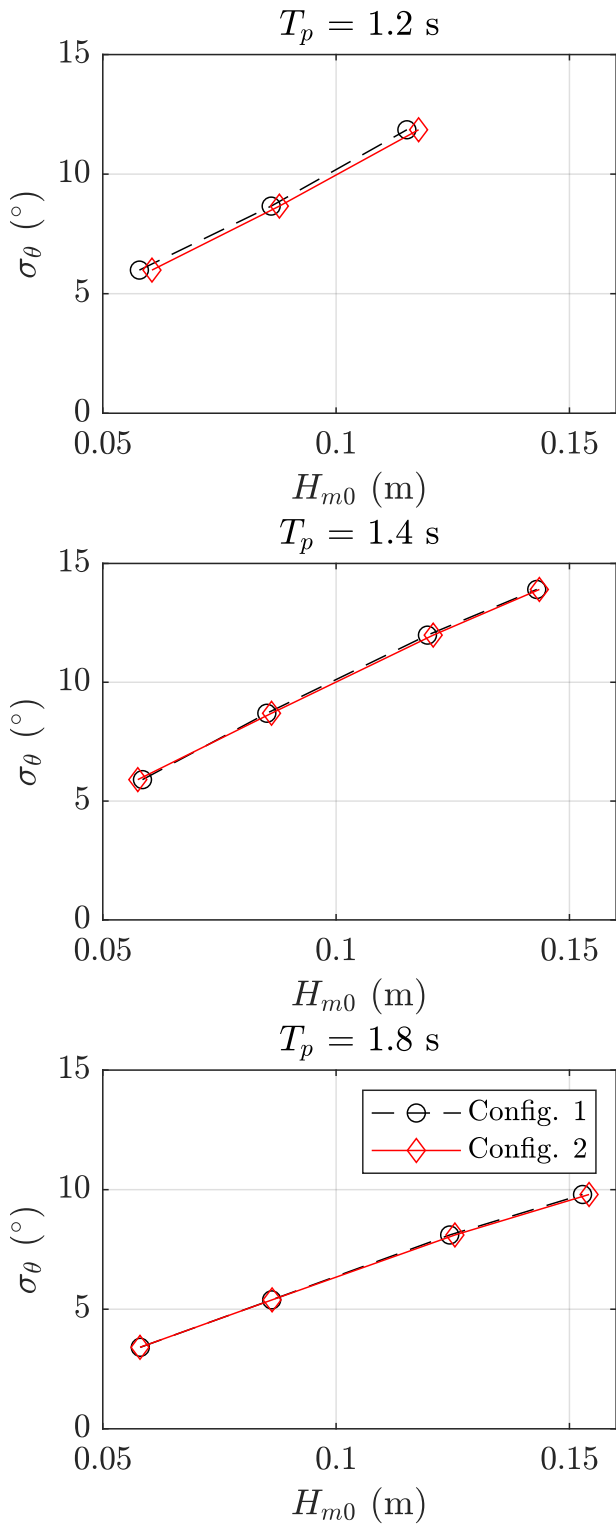


Fig. 11. Standard deviation of hinge angle as a function of H_{m0} for different values of T_p

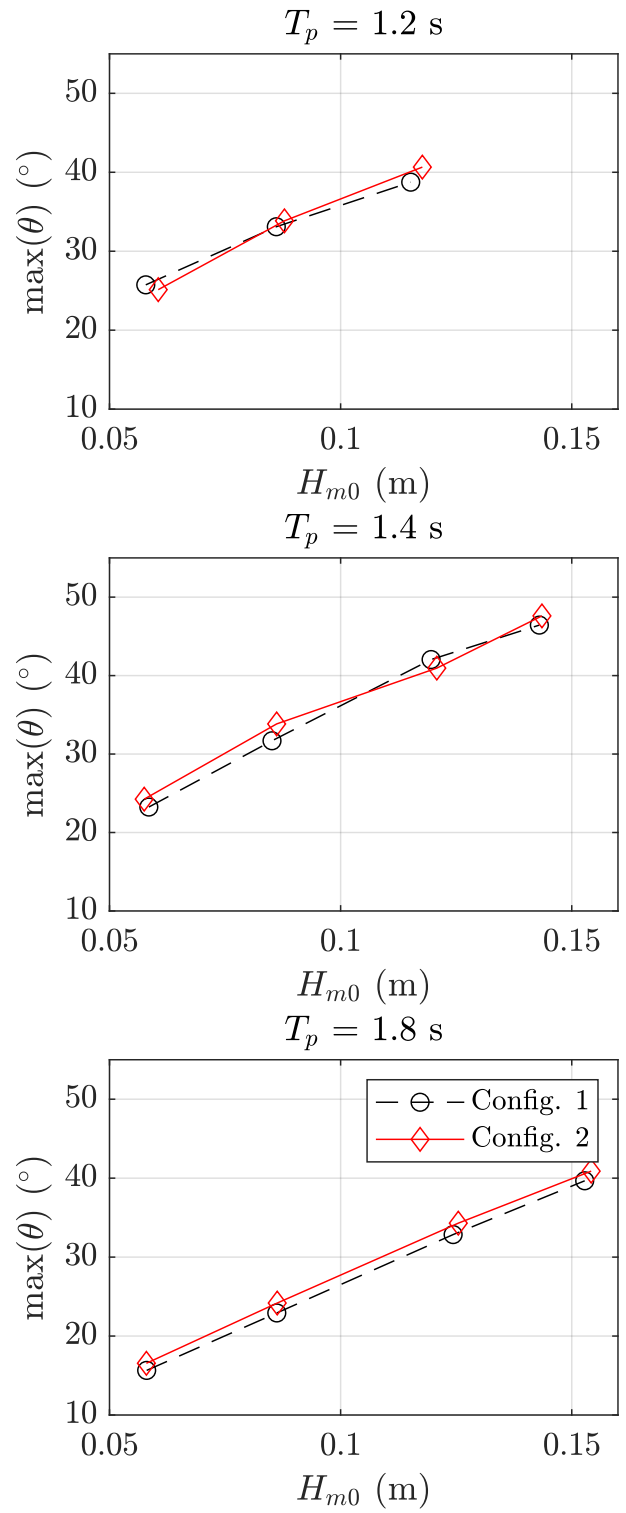
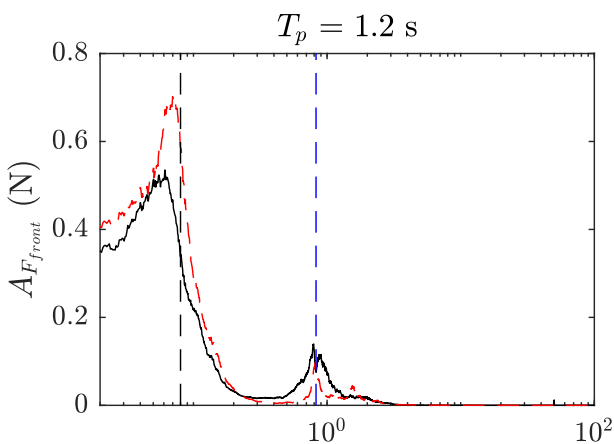


Fig. 10. Maximum hinge angle as a function of H_{m0} for different values of T_p



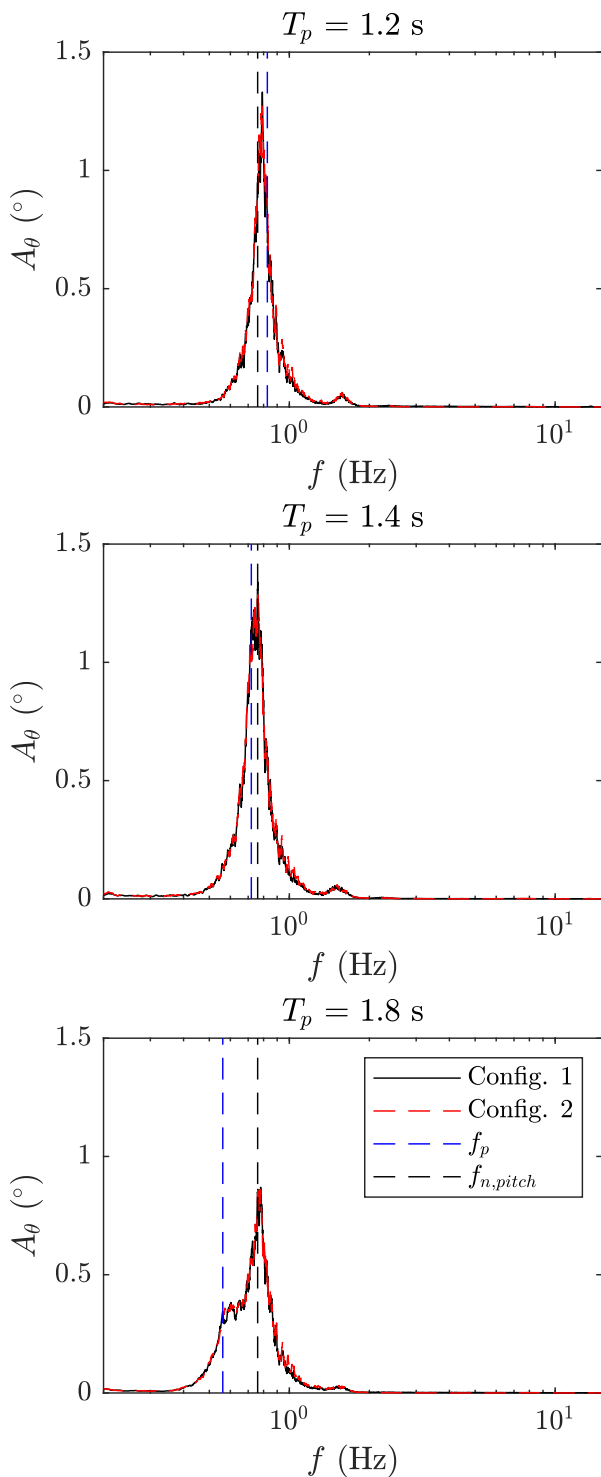


Fig. 13. Amplitude spectra of hinge angle shown for the maximum H_{m0} value for each T_p (cases 7, 10 and 11). The peak wave frequency and theoretical surge natural frequency are indicated by blue and black dashed lines respectively

ACKNOWLEDGEMENT

Funding through the EPSRC, UK MoorWEC grant EP/V039946/1 is gratefully acknowledged. The authors would like to thank Federica Buriani and the members of the University of Plymouth COAST Laboratory for their help delivering the experiments, and would like to thank Paul Nicholson at University of Manchester for their support instrumenting the model.

REFERENCES

- [1] K. Gunn and C. Stock-Williams, "Quantifying the global wave power resource," *Renewable Energy*, vol. 44, pp. 296–304, 2012. [Online]. Available: <https://doi.org/10.1016/j.renene.2012.01.101>
- [2] B. Paduano, G. Giorgi, R. P. Gomes, E. Pasta, J. C. Henriques, L. M. Gato, and G. Mattiazzo, "Experimental validation and comparison of numerical models for the mooring system of a floating wave energy converter," *Journal of Marine Science and Engineering*, vol. 8, no. 8, p. 565, 2020. [Online]. Available: <https://doi.org/10.3390/jmse8080565>
- [3] J. Davidson and J. V. Ringwood, "Mathematical modelling of mooring systems for wave energy converters—a review," *Energies*, vol. 10, no. 5, p. 666, 2017. [Online]. Available: <https://doi.org/10.3390/en10050666>
- [4] E. C. Moreno and P. Stansby, "The 6-float wave energy converter m4: Ocean basin tests giving capture width, response and energy yield for several sites," *Renewable and Sustainable Energy Reviews*, vol. 104, pp. 307–318, 2019. [Online]. Available: <https://doi.org/10.1016/j.rser.2019.01.033>
- [5] P. Stansby, S. Draycott, G. Li, C. Zhao, E. C. Moreno, A. Pillai, and L. Johannig, "Experimental study of mooring forces on the multi-float wec m4 in large waves with buoy and elastic cables," *Ocean Engineering*, vol. 266, p. 113049, 2022. [Online]. Available: <https://doi.org/10.1016/j.oceaneng.2022.113049>
- [6] P. Stansby and E. C. Moreno, "Hydrodynamics of the multi-float wave energy converter m4 with slack moorings: Time domain linear diffraction-radiation modelling with mean force and experimental comparison," *Applied Ocean Research*, vol. 97, p. 102070, 2020. [Online]. Available: <https://doi.org/10.1016/j.apor.2020.102070>
- [7] K. Hasselmann *et al.*, "Measurements of wind-wave growth and swell decay during the joint north sea wave project (jonswap)." *Ergaenzungsheft zur Deutschen Hydrographischen Zeitschrift, Reihe A*, 1973.
- [8] L. Zhang, P. Stansby, and S. Draycott, "Data-driven design optimisation of the mooring system for a multi-float wave energy converter using system identification techniques," *Submitted to: Mechanical Systems and Signal Processing*, 2025. [Online]. Available: <http://dx.doi.org/10.2139/ssrn.4844710>